Naive parton picture for kaon color transparency in $A(e, e'K^+)$*

Kook-Jin Kong[1†] Tae Keun Choi[2‡] Byung-Geel Yu[1,3§]

[1]Research Institute of Basic Science, Korea Aerospace University, Goyang 10540, Korea
[2]Department of Physics and Engineering Physics, Yonsei University, Wonju 26493, Korea
[3]Center for Exotic Nuclear Studies, Institute for Basic Science, Daejeon 34126, Korea

Abstract: Nuclear transparency in the electronuclear reaction $A(e,e'K^+)$ is investigated in parallel with our previous study of pion transparency in Phys. Rev. C **111**, 064608 (2025). Based on an extended Glauber framework that incorporates shadowing from the initial-state two-step process, kaon color transparency (CT) is analyzed to show that the steeper Q^2 dependence observed for kaon CT, compared with the pion case, is more naturally described by the naive parton model (NPM) than by the quantum diffusion model (QDM). The inclusion of initial-state shadowing further reduces the transparency and improves the agreement with the experimental data. The Q^2 and A dependences of the kaon transparency are presented up to $Q^2 = 10$ GeV$^2/c^2$, together with the corresponding $\alpha(Q^2)$ and the supplementary ratio T_A/T_C, for comparison with the Jefferson Lab (JLab) data obtained with the 6-GeV electron beam on ^{12}C, ^{63}Cu, and ^{197}Au nuclei.

Keywords: Color transparency, Kaon electroproduction, Nuclear transparency, Glauber model

DOI: 10.1088/1674-1137/ae6b20 **CSTR:**

I. INTRODUCTION

Nuclear transparency is a particularly useful observable for studying hadron propagation in nuclei and, at sufficiently large momentum transfer, the onset of color transparency (CT) in QCD [1, 2]. In the conventional hadronic picture, the attenuation of the ejectile is governed by its interactions with the nuclear medium, whereas CT is associated with the production of a small-size color-singlet configuration whose interaction with surrounding nucleons is reduced during the early stage of its expansion [1, 2]. Meson electroproduction is especially attractive in this respect, since CT is generally expected to set in more favorably for $q\bar{q}$ systems than for baryons, and the JLab pion-transparency measurements indeed revealed a systematic rise of the transparency with Q^2 over a broad range of nuclei [2–4].

Kaon electroproduction on nuclei is of particular interest in this context. Compared with the pion sector, dedicated studies of kaon transparency remain rather limited, even though the K^+ channel offers a natural opportunity to test CT in the strangeness sector [2, 5, 6]. Experimentally, Nuruzzaman *et al.* extracted nuclear transparencies from $A(e,e'K^+)$ on ^{12}C, ^{63}Cu, and ^{197}Au at $Q^2 = 1.1$, 2.2, and 3.0 GeV^2 [5]. The extracted effective in-medium kaon-nucleon cross sections were found to be smaller than the corresponding free-space values inferred from simple geometrical attenuation models [5]. On the theory side, Das showed that a conventional treatment based on free K^+N cross sections underestimates the measured transparency, whereas the introduction of a distance-dependent effective kaon–nucleon cross section, simulating CT, leads to a substantially improved description [6].

The present work is motivated by the observation that the standard Glauber framework, widely used in semiclassical analyses of meson transparency and CT [1, 7], need not exhaust all relevant reaction mechanisms in electroproduction on nuclei. In our previous study of pion transparency, we went beyond the conventional Glauber treatment by incorporating the shadowing generated by the initial-state two-step process associated with the $\gamma^* \to \rho^0$ fluctuation [8]. We found that, although the usual Glauber treatment supplemented with CT reproduces the gross Q^2 dependence, it tends to overestimate the measured pion transparency, whereas the additional vector-meson-induced shadowing leads to a substantially better description of the JLab $A(e,e'\pi^+)$ data for ^{12}C, ^{27}Al, ^{63}Cu, and ^{197}Au [8]. This naturally motivates a corresponding reexamination of kaon transparency, where the interplay of final-state CT and initial-state shadowing

Received 26 March 2026; Accepted 7 May 2026

* This work was supported by the National Research Foundation of Korea (NRF) under Grant No. NRF-2022R1A2B5B01002307 and by the Institute for Basic Science (IBS-R031-D1)

† E-mail: kong@kau.ac.kr
‡ E-mail: tkchoi@yonsei.ac.kr
§ E-mail: bgyu@kau.ac.kr

may also be relevant.

More microscopic descriptions of nuclear attenuation and CT certainly exist, including the Green-function/path-integral approach of Kopeliovich and collaborators [9], the relativistic multiple-scattering Glauber framework of the Ghent group [10], the semiclassical treatments of Larionov and collaborators [11], and coupled-channel transport calculations in GiBUU [12]. While these approaches are valuable for a more dynamical treatment of the reaction mechanism, their practical implementation generally involves substantially greater complexity and additional model dependence associated with intermediate-state propagation, multichannel couplings, and reaction-specific ingredients [9–12]. For the present purpose, namely to identify the dominant mechanisms governing kaon transparency in a form that can be confronted directly with the existing data, a transparent phenomenological framework is particularly useful. In such dynamical approaches, Fermi motion and Pauli blocking can influence the quantitative extraction of attenuation, although their roles are different: the former mainly smears the initial quasifree kinematics, whereas the latter restricts the available baryonic final states [4, 5]. In the present kaon channel, Pauli-blocking effects are expected to be less direct than in pionic channels, since the produced K^+ is a boson and the associated hyperon is not Pauli blocked by the nucleon Fermi sea [13].

Motivated by these considerations, we revisit nuclear transparency in $A(e,e'K^+)$ within an extended Glauber framework that includes both final-state CT effects through a reduced effective kaon–nucleon cross section and initial-state shadowing associated with vector-meson fluctuations of the virtual photon. Our aim is to determine how far the existing kaon-transparency data can be understood from the interplay of these two mechanisms in a simple phenomenological description, and to compare the kaon case with our previous pion-transparency analysis in order to discuss the onset of CT in the strangeness sector.

This paper is organized as follows. In Sec. II, we formulate the NPM [14] alongside the QDM for analyzing the Q^2 dependence of kaon transparency in the reaction $A(e,e'K^+)$, based on the extended Glauber framework developed in Ref. [8]. The shadowing effect introduced in Ref. [8] is included as an additional mechanism that further reduces the apparent kaon transparency. Within this framework, we reproduce the observed Q^2 and A dependences of the nuclear transparency T_A and evaluate the corresponding Q^2 dependence of the parameter α. As a supplementary observable, we also present the ratio T_A/T_C, i.e. the transparency normalized to that of ^{12}C. These results are then compared with the JLab data obtained with the 6-GeV electron beam. Section III contains a summary and concluding remarks.

II. MODELS FOR DATA ANALYSIS

The reaction $A(e,e'K^+)$ proceeds via the elementary subprocess $\gamma^*(k)+p(p)\to K^+(p_K)\Lambda(p')$ (or Σ^0), with the relevant kinematic quantities listed in Table 1. In the present work, the nuclear transparency T_A is evaluated within an extended Glauber framework that incorporates both the final-state attenuation of the outgoing kaon and the initial-state shadowing associated with the two-step process. The resulting expression is given by [8]

$$T_A=\frac{1}{A}\int d^2b\int_{-\infty}^{\infty}dz\varrho(b,z)\times\exp\left[-\sigma_{\phi N}\int_{z-l_c}^{z}dz'\varrho(b,z')-\int_{z}^{\infty}dz'\,\sigma_{KN}^{\rm eff}(z')\varrho^*(b,z')\right]. \tag{1}$$

Here ϱ and ϱ^* denote the nuclear density distributions of the target nucleus A and the recoiling $(A-1)$ system, respectively. In the present calculation we employ a Woods–Saxon distribution for the nuclear density with the same prescription as in Ref. [8].

Equation (1) makes the reaction sequence explicit. The first exponential factor represents the shadowing correction in the initial state, where the virtual photon fluctuates into a vector meson at $z-l_c$ and propagates over the coherence length before the kaon is produced at z to scatter off a nearby nucleon [16–18]. The second factor describes the attenuation of the outgoing kaon through the effective kaon–nucleon cross section $\sigma_{KN}^{\rm eff}(z)$ along its path through the nucleus. Since the virtual photon couples to the kaon channel through the fluctuation $\gamma^*\to\phi(1020)\to K^+K^-$, the coherence length is given by

$$l_c=\frac{2\nu}{Q^2+m_\phi^2}, \tag{2}$$

and the corresponding values are listed in Table 1 for the respective Q^2 values.

In the present framework, the elementary input for the hadronic attenuation is crucial to determining the Q^2 dependence of the transparency. In particular, the size of σ_{KN} governs the overall strength of the final-state interaction, while the choice of $\sigma_{\phi N}$ controls the magnitude of the initial-state shadowing. The cross section $\sigma_{\phi N}$ is constrained only indirectly through photoproduction data and nuclear-transparency analyses, with typical free-space estimates lying in the range of about 10–20 mb [19–22]. In the present calculation, we use the K^+N total cross sections quoted by the PDG [15], as listed in Table 1, and adopt $\sigma_{\phi N}=18$ mb following Ref. [23].

To implement color transparency in the Glauber framework, one needs a distance-dependent effective kaon–nucleon cross section. A standard choice is the quantum diffusion model (QDM), whose applicability has

Table 1. Kinematical variables Q^2 (GeV$^2/c^2$), W (GeV), E_e (GeV), θ_e (deg), E'_e (GeV), x_B, and p_K (GeV/c) for kaon electroproduction, together with the quantities relevant to the JLab measurement of kaon transparency in the range $0.5 \le Q^2 \le 10$ GeV$^2/c^2$ [5]. Also shown are the coherence length l_c (fm) with m_ϕ in Eq. (2), the formation length $l_f^{\rm NPM}$ (fm) with $R_K = 0.58$ fm in Eq. (3), and the formation length $l_f^{\rm QDM}$ (fm) with $\Delta M^2 = 0.3$ GeV^2 in Eq. (4). For each kinematical setting, the total cross section $\sigma_{KN}(p_K)$ is assigned from the PDG [15] K^+N total-cross-section values at the corresponding kaon momentum p_K. Since the variation over the relevant momentum range is weak, this amounts in practice to using piecewise-constant values, as listed in the last column of the table. Throughout this work we use $\sigma_{\phi N} = 18$ mb for the shadowing correction associated with the two-step process [8].

Q^2	W	E_e	θ_e	E'_e	x_B	p_K	l_c	$l_f^{\rm NPM}$	$l_f^{\rm QDM}$	σ_{KN}
0.55	2.28	3.4	26	0.8	0.11	2.24	0.65	2.7	2.95	
0.69	2.25	3.5	27	0.9	0.14	2.22	0.60	2.68	2.93	
0.77	2.25	3.68	26	1.04	0.16	2.26	0.58	2.71	2.97	18
0.92	2.26	3.85	27	1.1	0.18	2.36	0.56	2.83	3.10	
1.05	2.26	4.02	27	1.2	0.2	2.41	0.54	2.89	3.17	
1.10	2.26	4.02	27.76	1.19	0.21	2.42	0.53	2.9	3.18	
2.15	2.21	5.01	28.85	1.73	0.35	2.74	0.41	3.27	3.60	
3.0	2.14	5.01	37.77	1.43	0.45	2.89	0.35	3.45	3.81	17
3.91	2.26	5.77	40.38	1.42	0.48	3.61	0.35	4.29	4.76	
4.69	2.25	5.77	52.67	1.03	0.53	3.90	0.33	4.62	5.14	
5.0	2.43	11.0	16.28	5.67	0.5	4.57	0.35	5.4	6.00	
6.5	2.74	11.0	22.13	4.01	0.5	6.25	0.37	7.37	8.23	18
8.0	3.02	11.0	32.37	2.34	0.49	7.94	0.38	9.34	10.44	
9.5	3.09	11.0	47.71	1.32	0.52	8.89	0.36	10.46	11.69	

been examined extensively in the pion and ρ^0 sectors [2, 4, 10, 24–26]. For the kaon case, however, the observed Q^2 dependence appears steeper than what is naturally generated by the usual QDM parametrization, even when the mass parameter in the formation length is readjusted [6]. This motivates us to consider, in parallel, the naive parton model (NPM), which offers a simple benchmark for the space-time expansion of a compact $q\bar{q}$ configuration.

In the naive parton picture, the suppression of the effective cross section is estimated from the reduced transverse size of the initially produced configuration, $\sigma_{KN}^{\rm eff}/\sigma_{KN} \sim x_t^2/\langle x_t^2\rangle \sim \langle k_t^2\rangle/Q^2$, where x_t denotes the transverse size of the $q\bar{q}$ configuration. Meanwhile, partons separating at velocity c propagate over the longitudinal distance $z \sim (E/m)x_t$, which defines the formation length after relativistic dilation [14]. This gives

$$l_f^{\rm NPM} = \left(\frac{E_K}{m_K}\right) R_K , \tag{3}$$

where R_K denotes the transverse size associated with the forming kaon and is here taken to be the kaon charge radius. This choice should not be interpreted as a strict identification of the initially produced compact $q\bar{q}$ configuration with the physical kaon, but rather as a practical estimate of the relevant hadronic length scale without introducing an additional adjustable parameter. In contrast, the QDM associates the expansion length with the inverse energy difference between hadronic states [2], leading to

$$l_f^{\rm QDM} = \frac{2p_K}{\Delta M^2} . \tag{4}$$

The effective cross section that accommodates both models can then be written in the unified form

$$\sigma_{KN}^{\rm eff}(z;Q^2,p_K) = \sigma_{KN}(p_K)\left[\theta(z-l_f) + \left\{\frac{n^2\langle k_t^2\rangle}{Q^2}\left(1-\left(\frac{z}{l_f}\right)^{\tau}\right)+\left(\frac{z}{l_f}\right)^{\tau}\right\}\theta(l_f-z)\right], \tag{5}$$

where $\tau = 2$ corresponds to the NPM and $\tau = 1$ to the QDM, with $n = 2$ for the $q\bar{q}$ configuration. Equation (5) is the central ingredient of the present analysis, since it embeds the CT effect directly into the nuclear absorption through the explicit Q^2 dependence of $\sigma_{KN}^{\rm eff}$. In QCD, a virtual photon with larger Q^2 selects a compact color-singlet $q\bar{q}$ configuration with a small transverse size, whose interaction with the surrounding nucleons is suppressed by color screening. Since the effective interaction strength decreases with the transverse size of the

compact configuration, the nuclear absorption becomes weaker as Q^2 increases. Therefore, once ordinary nuclear effects such as Glauber attenuation based on the free-space cross section and shadowing are properly taken into account, a nontrivial Q^2 dependence of the effective absorption can be regarded as a direct signature of the onset of color transparency [27−29].

In the numerical calculation, we use $\langle k_t^2\rangle^{1/2} \simeq 0.35$ GeV/c for the quark transverse momentum in the kaon. For each kinematical setting, $\sigma_{KN}(p_K)$ is assigned from the PDG K^+N total-cross-section values at the corresponding kaon momentum p_K [15]. Because the variation over the relevant momentum range is weak and no pronounced resonance structure appears there, this is implemented in practice as piecewise-constant values, as listed in Table 1.

For the NPM calculation we use $R_K = 0.58$ fm in Eq. (3), corresponding to the measured kaon charge radius, $\langle R_K^2\rangle = 0.34 \pm 0.05$ fm^2, reported in Ref. [30]. For the QDM estimate we take $\Delta M^2 = 0.3$ GeV^2, as advocated in Ref. [6], and compare it with the more commonly used value $\Delta M^2 = 0.7$ GeV^2, which is often favored in pion-transparency analyses.

Figure 1 illustrates the ratio $\sigma_{KN}^{\rm eff}/\sigma_{KN}$ in Eq. (5) as a function of the propagation distance z at $Q^2 = 3.0$ GeV$^2/c^2$ and $p_K = 2.89$ GeV/c. The dotted, dashed, solid, and dash-dotted curves correspond to the formation lengths $l_f = 1.63$ fm with $\Delta M^2 = 0.7$ GeV^2 and $l_f = 3.81$ fm with $\Delta M^2 = 0.3$ GeV^2 from the QDM, and to $l_f = 3.45$ fm with $R_K = 0.58$ fm and $l_f = 4.16$ fm with $R_K = 0.7$ fm from the NPM, respectively. The figure makes the difference between the two scenarios transparent: the QDM gives a linear rise with z/l_f, whereas the NPM yields a quadratic increase. The contribution obtained with $\Delta M^2 = 0.7$ GeV^2 is therefore noticeably weaker than the others.

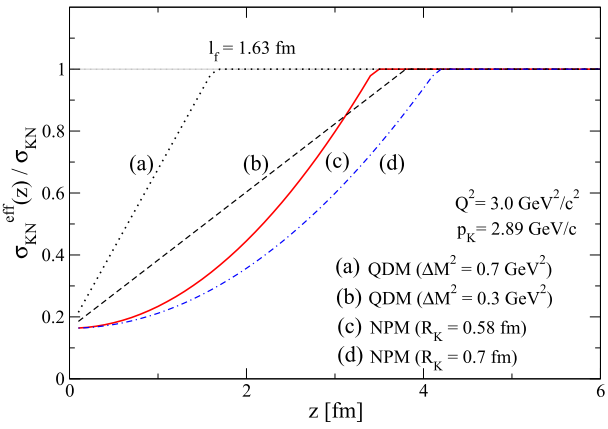

Fig. 1. (color online) Ratio $\sigma_{KN}^{\rm eff}/\sigma_{KN}$ in Eq. (5) as a function of the propagation distance z at $Q^2 = 3.0$ GeV$^2/c^2$ and $p_K = 2.89$ GeV/c. The four labeled curves correspond to the two QDM cases, $l_f = 1.63$ fm with $\Delta M^2 = 0.7$ GeV^2 and $l_f = 3.81$ fm with $\Delta M^2 = 0.3$ GeV^2, and the two NPM cases, $l_f = 3.45$ fm with $R_K = 0.58$ fm and $l_f = 4.16$ fm with $R_K = 0.7$ fm. The corresponding formation lengths are obtained from Eqs. (3) and (4) for the NPM and QDM, respectively.

The calculated Q^2 dependence of the transparency T_A is shown in Fig. 2 for ^{12}C, ^{63}Cu, and ^{197}Au. The solid curves are obtained from the extended Glauber model of Eq. (1), where the final-state CT effect is described by the NPM with $R_K = 0.58$ fm and the initial-state shadowing is evaluated with $\sigma_{\phi N} = 18$ mb. The dashed curves show the NPM result without shadowing. The dotted curves correspond to the pure Glauber baseline, where neither CT nor shadowing is included, and the dash-dotted curves display the shadowing correction to that baseline. For comparison, panel (a) also shows the QDM predictions with $\Delta M^2 = 0.3$ and 0.7 GeV^2 for the ^{197}Au target.

Several features deserve emphasis. First, the inclusion of shadowing lowers the transparency systematically and improves the overall agreement with the data. Second, the QDM with the more conventional choice $\Delta M^2 = 0.7$ GeV^2 fails to reproduce the observed rise of the kaon transparency and is therefore not retained in the subsequent comparison. Third, although the QDM with $\Delta M^2 = 0.3$ GeV^2 becomes comparable to the NPM once shadowing is included, this choice is less well constrained physically than the use of the experimental kaon charge radius in the NPM. In addition, the steeper Q^2 de-

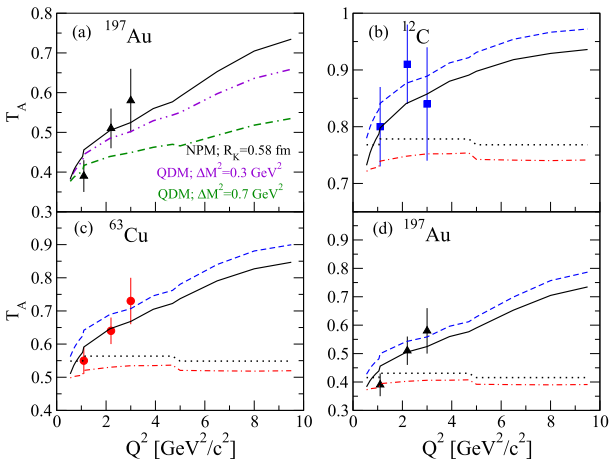

Fig. 2. (color online) Q^2 dependence of the nuclear transparency T_A in ^{12}C, ^{63}Cu, and ^{197}Au. The solid curves show the result of the extended Glauber calculation in Eq. (1), where the NPM with $R_K = 0.58$ fm is used and the shadowing effect is evaluated with $\sigma_{\phi N} = 18$ mb. The dashed curves show the NPM result without shadowing. The dotted curves correspond to the pure Glauber calculation without NPM or shadowing, and the dash-dotted curves indicate the shadowing correction to that baseline. For comparison, panel (a) also shows the QDM predictions for $\Delta M^2 = 0.3$ GeV^2 and 0.7 GeV^2, represented by the dash-dot-dotted and dash-dash-dotted curves, respectively. The data are taken from Ref. [5].

pendence of the data is more naturally reproduced by the quadratic growth of $\sigma_{KN}^{\rm eff}(z;Q^2)$ in the NPM than by the linear rise characteristic of the QDM.

Figure 3 presents the ratio T_A/T_C, where the transparency of a heavier target is normalized to that of ^{12}C. Although normalization to deuterium is experimentally advantageous, since the deuteron provides an approximately isoscalar *pn* system and can partially cancel effects from proton–neutron imbalance, nuclear binding, and Fermi motion, such a normalization is not entirely natural within the present framework. The Glauber model used here is formulated for nuclei with sufficiently large A and nearly spherical density distributions, rather than for the weakly bound and nonspherical deuteron. For this reason, we also consider the ratio T_A/T_C, for which the normalization to ^{12}C is better matched to the conditions under which the present Glauber approach is expected to be reliable. Unlike deuterium, however, ^{12}C is not a nearly transparent reference system, and its bound nucleons cannot be regarded as quasi-free, which is a limitation of the ^{12}C normalization. Nevertheless, because ^{12}C is already a finite nucleus with a well-defined density distribution, one may incorporate corrections associated with short-range correlations (SRC) and nuclear attenuation, which can partly compensate for these effects. For this reason, the ^{12}C-normalized ratio remains a meaningful supplementary observable within the present model. Within the present framework, the shadowing-corrected NPM prediction (solid) exhibits a steeper Q^2 dependence than the corresponding QDM prediction (dash-dot-dotted) for both ^{63}Cu and ^{197}Au.

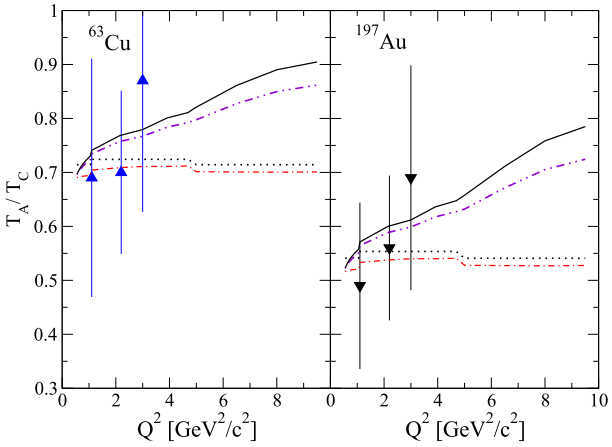

Fig. 3. (color online) Q^2 dependence of the ratio T_A/T_C obtained by normalizing the transparency of each target nucleus to that of ^{12}C. The solid curves represent the ratio predicted by the extended Glauber calculation, including shadowing and the NPM, with the same notation as in Fig. 2. The dash-dot-dotted curves show the corresponding result from the extended Glauber calculation including shadowing and the QDM with $\Delta M^2 = 0.3$ GeV^2. The data are taken from Ref. [5].

The dependence of T_A on the mass number A is shown in Fig. 4 for fixed values of Q^2. From top to bottom, the panels correspond to $Q^2 = 1.1$, 2.2, and 3.0 GeV$^2/c^2$, respectively. As expected, the transparency decreases rapidly with increasing A, reflecting the longer path of the outgoing kaon through nuclear matter in heavier systems. The comparison between the solid and dashed curves isolates the role of the initial-state shadowing, while the dash-dot-dotted curve in the middle panel shows the QDM result for comparison.

A related characterization of the nuclear dependence is provided by the parameter $\alpha(Q^2)$, defined through

$$T_A = A^{\alpha(Q^2)-1}, \tag{6}$$

which follows from the scaling form $\sigma_A = A^{\alpha}\sigma_N$. A deviation of α from unity therefore signals a nuclear effect beyond a simple incoherent sum over free nucleons. The extraction of $\alpha(Q^2)$ has previously been discussed for pion transparency [4] and for the kaon case in Ref. [5].

The result is shown in Fig. 5. In hadron–nucleus scattering, the empirical value $\alpha \simeq 0.78$ extracted from K^+–nucleus data corresponds to an ordinary absorptive

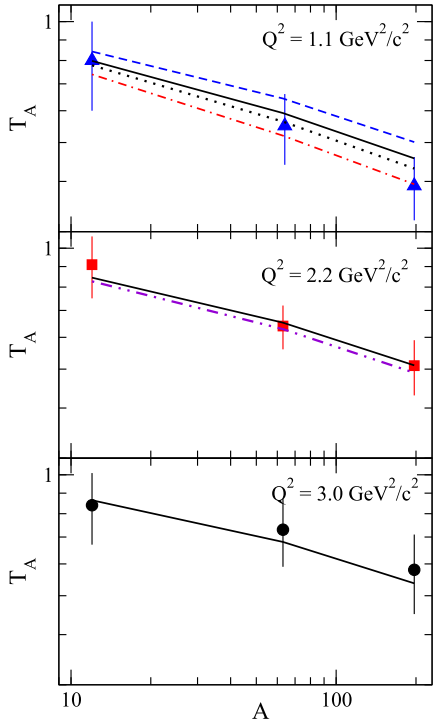

Fig. 4. (color online) A-dependence of T_A at fixed Q^2. From top to bottom, the panels correspond to $Q^2 = 1.1$, 2.2, and 3.0 GeV$^2/c^2$, respectively. The solid and dashed curves show the calculations with and without shadowing, with the same notation as in Fig. 2. For comparison, the QDM prediction at $Q^2 = 2.2$ GeV$^2/c^2$ is shown by the dash-dot-dotted curve in the middle panel. The data are taken from Ref. [5].

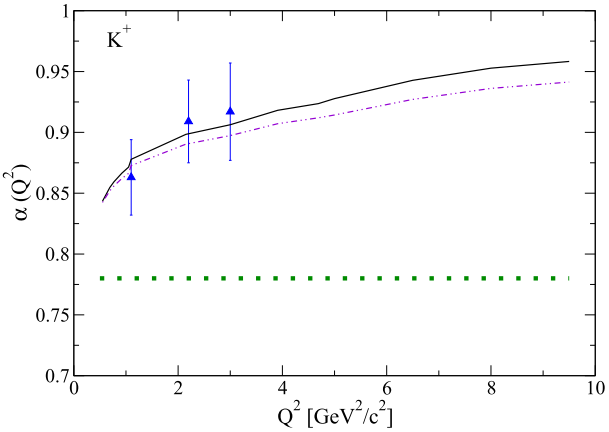

Fig. 5. (color online) Q^2 dependence of α for the nuclear transparency T_A. The parameter α is extracted by averaging over the JLab data for the three target nuclei. The dash-dot-dotted curve shows the QDM result for comparison, and the thick dotted line denotes the approximately constant value of α extracted from K^+–nucleus scattering [31]. The data are taken from Ref. [5].

regime, well below the volume-scaling limit $\alpha = 1$, where T_A is independent of A, but still above the opaque-nucleus limit $\alpha = 2/3$ discussed by Carroll *et al.* [31]. By contrast, the rise of $\alpha(Q^2)$ from about 0.85 to 0.95 in $A(e,e'K^+)$ indicates a substantial reduction of attenuation, so that the transparency shows a progressively weaker A dependence and approaches more volume-like propagation in the nucleus.

III. CONCLUSION

We have investigated nuclear transparency in the reaction $A(e,e'K^+)$ for the representative nuclei ^{12}C, ^{63}Cu, and ^{197}Au in order to analyze the onset of kaon color transparency. Within an extended Glauber framework over the range $0.55 \le Q^2 \le 10$ GeV$^2/c^2$, we included both the shadowing associated with the two-step process in the initial state and the color-transparency effect in the final state, described by either the QDM or the NPM, and compared the results with the available JLab data obtained with the 6-GeV electron beam.

Compared with the pion case under similar kinematic conditions, strangeness production involves a smaller hadronic attenuation because the relevant K^+N cross section is weaker than the corresponding πN one over the momentum range of interest. In this situation, the standard QDM parametrization constrained by the pion sector does not account satisfactorily for the kaon data unless the mass parameter is reduced to $\Delta M^2 = 0.3$ GeV^2. By contrast, the NPM, implemented through the quadratic growth of $\sigma_{KN}^{\rm eff}(z;Q^2)$ and supplemented by the initial-state shadowing correction, reproduces the observed Q^2 dependence of T_A, the target-normalized ratio T_A/T_C, and the overall A dependence rather well. The present analysis therefore indicates that the existing kaon-transparency data favor the NPM-type expansion scenario over the standard QDM parametrization, and that the steeper Q^2 dependence of kaon transparency is more naturally accommodated by the NPM.

A more microscopic treatment within a dynamical transport framework would nevertheless be valuable. To our knowledge, a dedicated study of exclusive kaon transparency in $A(e,e'K^+)$ within a full GiBUU-type or related dynamical transport framework has not yet been established at the same level. In such approaches, effects such as Fermi motion, multistep collisions, channel coupling, and collision broadening may modify the quantitative attenuation, but are unlikely by themselves to generate the steep monotonic Q^2 dependence observed in the present data. We therefore expect that a full dynamical transport calculation may change the quantitative values, but that the main qualitative conclusion of the present work is likely to remain robust. The present results also show that initial-state shadowing is not negligible even in this energy regime and should be included together with final-state color transparency when discussing the onset of CT in strangeness production off nuclei.

References

[1] L. L. Frankfurt, G. A. Miller, and M. Strikman, Ann. Rev. Nucl. Part. Sci. **44**, 501 (1994)
[2] D. Dutta, K. Hafidi, and M. Strikman, Prog. Part. Nucl. Phys. **69**, 1 (2013)
[3] B. Clasie *et al.*, Phys. Rev. Lett. **99**, 242502 (2007)
[4] X. Qian *et al.*, Phys. Rev. C **81**, 055209 (2010)
[5] Nuruzzaman *et al.*, Phys. Rev. C **84**, 015201 (2011)
[6] S. Das, Phys. Rev. C **100**, 035203 (2019)
[7] A. Larson, G. A. Miller, and M. Strikman, Phys. Rev. C **74**, 018201 (2006)
[8] T. K. Choi, K.-J. Kong, and B.-G. Yu, Phys. Rev. C **111**, 064608 (2025)
[9] B. Z. Kopeliovich, J. Nemchik, A. Schäfer, and A. V. Tarasov, Phys. Rev. C **65**, 035201 (2002)
[10] W. Cosyn, M. C. Marti'nez, and J. Ryckebusch, Phys. Rev. C **77**, 034602 (2008)
[11] A. Larionov and M. Strikman, Particles **3**, 75 (2020)
[12] K. Gallmeister and U. Mosel, Physics **4**, 440 (2022)
[13] F. Garibaldi *et al.*, Phys. Rev. C **99**, 054309 (2019)
[14] G. R. Farrar, H. Liu, L. L. Frankfurt and M. I. Strikman, Phys. Rev. Lett. **61**, 686 (1988)
[15] S. Navas *et al.* (Particle Data Group), Phys. Rev. D **110**, 030001 (2024)
[16] T. H. Bauer, R. D. Spital, D. R. Yennie, and F. M. Pipkin, Rev. Mod. Phys. **50**, 261 (1978)
[17] D. R. Yennie, *Hadronic Interactions of Electrons and Photons: Proceedings of the 11th Session of the Scottish Universities Summer School in Physics, 1970*, edited by J.

Cumming and H. Osborn (Academic, New York, 1971), p. 321.
[18] J. Hüfner, B. Kopeliovich, and J. Nemchik, Phys. Lett. B **383**, 362 (1996).
[19] A. Sibirtsev, H.-W. Hammer, U.-G. Meißner, and A. W. Thomas, Eur. Phys. J. A **29**, 209 (2006)
[20] X. Qian *et al*. [CLAS Collaboration], Phys. Lett. B **680**, 417 (2009)
[21] S. Das, Phys. Rev. C **103**, 035205 (2021)
[22] Ph. Gubler, M. Ichikawa, T. Song, and E. Bratkovskaya, Phys. Rev. C **111**, 034908 (2025)
[23] S. D. Drell and J. S. Trefil, Phys. Rev. Lett. **16**, 552 (1966)
[24] A. Airapetian *et al*., Phys. Rev. Lett. **90**, 052501 (2003)
[25] L. El Fassi *et al*., Phys. Lett. B **712**, 326 (2012)
[26] A. B. Larionov, M. Strikman and M. Bleicher, Phys. Rev. C **93**, 034618 (2016)
[27] S. J. Brodsky and A. H. Mueller, Phys. Lett. B **206**, 685 (1988)
[28] P. Jain, B. Pire, J. P. Ralston, Phys. Rept. **271**, 67 (1996)
[29] B. Z. Kopeliovich, J. Nemchik, N. N. Nikolaev, and B. G. Zakharov, Phys. Lett. B **324**, 469 (1994)
[30] S. R. Amendolia *et al*., Phys. Lett. B **178**, 435 (1986)
[31] A. S. Carroll *et al*., Phys. Lett. B **80**, 319 (1979)